Characteristics of the Strong Ground Motion from the 24ᵗʰ August 2016 Amatrice Earthquake

MARTA PISCHIUTTA[1,*], AYBIGE AKINCI[1], LUCA MALAGNINI[1], ANDRE HERRERO[1]

[1]Istituto Nazionale di Geofisica e Vulcanologia, Sezione Roma 1,Via di Vigna Murata 605, 00143, Roma, Italy

marta.pischiutta@ingv.it*

Abstract

The 2016 August 24 Amatrice earthquake occurred at 03:36 local time in Central Apennines Italy with an epicentre at 43.36°E, 38.76°N, Istituto Nazionale di Geofisica e Vulcanologia (INGV), few kilometers north of the city of Amatrice. The earthquake ruptured a North-West (NW)–South-East (SE) oriented normal fault dipping toward the South-West (SW) (Scognamiglio et al., 2016). High values of peak ground acceleration (~0.92 g) were observed close to Amatrice (3 stations being few kilometer distances from the fault). The present study presents an overview of the main features of the seismic ground shaking during the Amatrice earthquake. We analyze the ground motion characteristics of the main shock in terms of peak ground acceleration (PGA), peak ground velocity (PGV) and spectral accelerations (SA, 5 per cent of critical damping). In order to understand the characteristics of the ground motions induced by Amatrice earthquake, we also study the source-related effects relative to the fault rupture directivity.

I. INTRODUCTION

On 24 August 2016, an earthquake occurred at 01:36 local time with an epicentre located close to Accumoli village, with an estimated magnitude Mw of 6.0 and its hypocentral at a depth of 8 km (http://cnt.rm.ingv.it /event/7073641). The causative fault is normal according to the Moment Tensor (MT) solution. It is due to the extensional tectonic regime in Central Apennines related to the opening of the Tyrrhenian back-arc basin. The earthquakes caused about 300 fatalities and diffuse building collapses in the towns of Amatrice and Arquata del Tronto, and in villages nearby, as an effect of the proximity of the causative fault and of the high vulnerability of old constructions in cobblestone. The main shock was followed by a seismic sequence with about 20 aftershocks with magnitude greater than 4.0 (Gruppo di Lavoro INGV, 2016). The earthquake occurred in the most seismically active part of Italy where several large earthquakes occurred over the last 700 years (http://emidius.mi.ingv.it/CPTI15-DBMI15/). In the same area an earthquake occurred on October 7, 1639 with similar intensity (equivalent magnitude 5.8), which is considered to be the strongest in Amatrice and its surrounding (Castelli et al. 2016). The epicentre of the Amatrice earthquake was located at about 35 km north of the destructive magnitude 6.3 earthquake hitting L'Aquila seven years ago in 2009.

The largest peak ground accelerations have been recorded at three closest stations of the Italian Accelerometric Network (RAN) (AMT, NRC and RQT) being up to 0.92 g at the AMT station (ran.protezionecivile.it/IT/index.php).

1

In this study we discuss the general characteristics of strong ground motion associated to the main shock in terms of ground motion parameters (PGA, PGV and PSA), and compare them with the outcome of Ground Motion Prediction Equations (GMPEs). In particular, we investigate the spatial and azimuthal distribution of peak ground motions, inferring the occurrence of a directivity effect.

II. OBSERVED GROUND MOTION AND GMPEs

We used data recorded by 98 accelerometric stations of the Italian strong motion network (RAN Rete Accelerometrica Nazionale which are equipped with Kinemetrics Episensor (FBA-3 200 Hz) and with ETNA 18 bits or K2-Makalu 24 bits digitizers.

The processed waveforms were downloaded from the European Strong Motion, ESM database (http://esm.mi.ingv.it; Luzi et al., 2016).

In **Figure 1** we show corrected acceleration, velocity and displacement traces of the main shock for two stations (AMT and NRC) closest to the fault rupture, at zero distance from the fault surface projection 1.4 and 2.7 km Joyner and Boore distance, R_{jb}, respectively see also map in **Figures 3** and **4**). The fault surface projection was derived by Cirella & Piatanesi (2016) inversion model. Station NRC showed similar PGA levels in the two horizontal components, in the order of 0.3 g, while station AMT shows relevant differences between EW and NS AMT components, with the largest peak of 0.92 g and 0.45 g respectively.

Figure 1. *Time series of acceleration, velocity and displacement (black colors indicate EW component and red NS component) from the main shock of the Amatrice seismic sequence, registered at stations: (a) NRC, (b) AMT.*
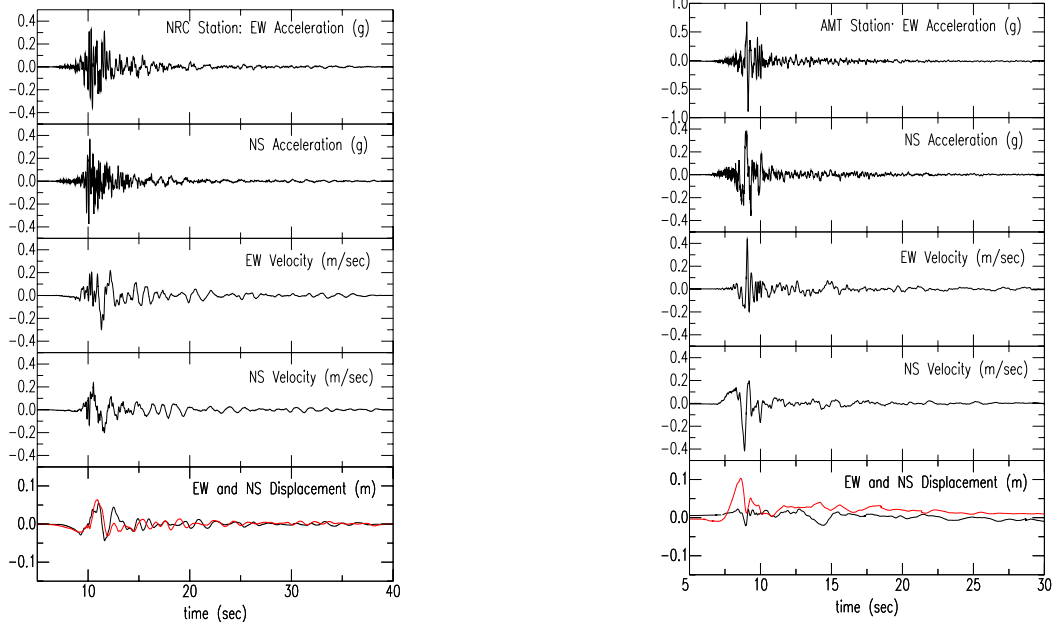
Furthermore, velocity and displacement time-histories highlight the presence of strong pulses at the beginning, possibly related to source effects. Such pulses are typical of near-fault motions. They transfer significant energy to buildings structural systems, and give a relevant contribution to their damage. At AMT and NRC stations, PGV reaches 44 and 29 cm/s, respectively. Measured horizontal peak acceleration, velocity and pseudo-spectral acceleration were compared with ground motion prediction equations (GMPEs) produced by several authors using both weak and strong motion

data: Boore & Atkinson, 2008 (BA08), Bindi et al. 2011 (ITA10), Malagnini et al., 2011 (MAL11). The BA08 model was developed within the context of the Next Generation Attenuation (NGA) models and used an extensive global strong-motion database. The latter is made of 1574 records from 58 main shocks in the distance range from 0 km to 400 km. Bindi et al. (2011) used 561 three-component waveforms from 107 earthquakes with moment magnitude M_w in the range 4.0–6.9, occurred in Italy from 1972 to 2007 and recorded by 206 stations at distances up to 100km. The Malagnini et al. (2011) GMPE is based on a data set of 12777 waveforms
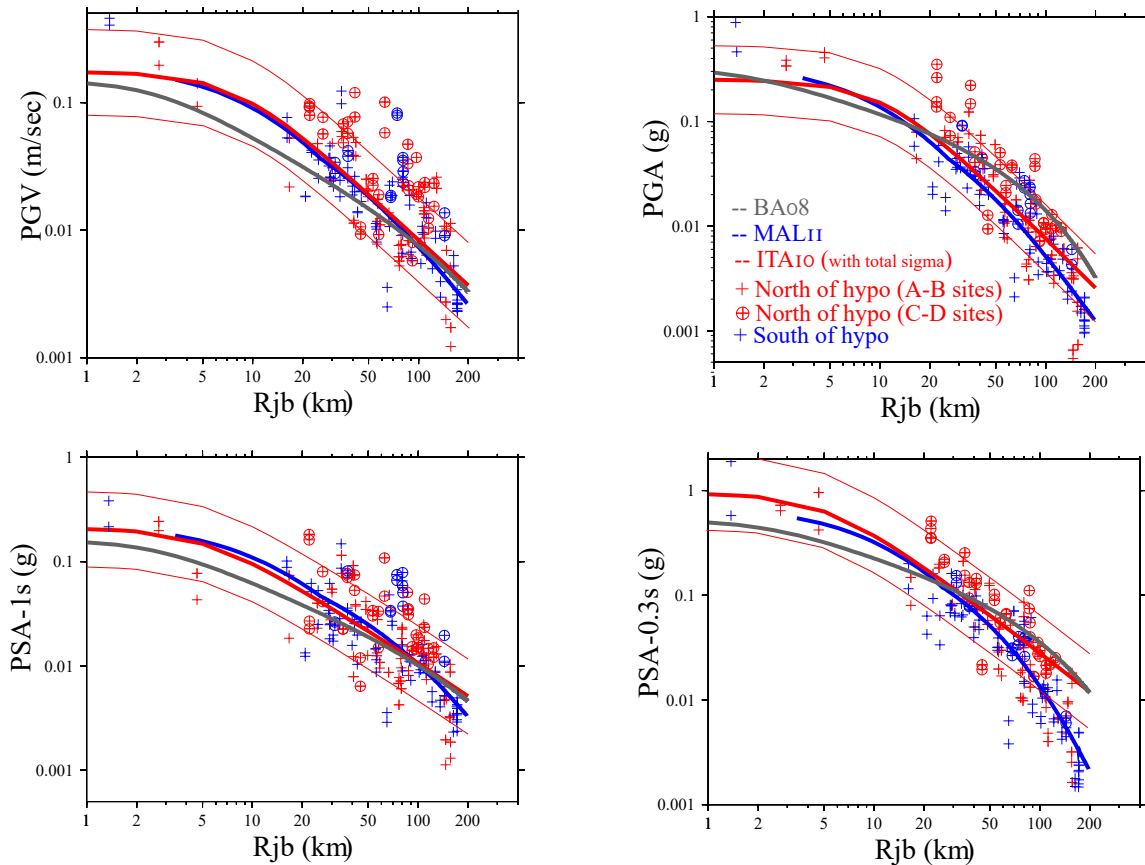
Figure 2. *Two horizontal components of PGA, PGV and PSA at 0.3 and 1 s compared with the ground-motion empirical predictive model of BA08, ITA10 and MAL11 as a function Rjb distances between 0 and 200 km.*

Red and blue symbols represent the observed PGA values in North/North-Western and South/South-Western sectors, respectively. Circles indicate "C" and "D" sites according to NTC08 Italian seismic code

from weak- and strong-motion recordings of 170 earthquakes (M_L >3) recorded during L'Aquila 2009-2010 seismic sequence.

In **Figure 2** we finally plot two horizontal components of PGA, PSA at 0.3 and 1.0 s and PGV values of the strong motion recordings as a function of the R_{jb} at the 98 considered stations of RAN network. They are compared with the values of the empirical GMPEs previously mentioned (BA08, ITA10, MAL11). Red crosses indicate stations located in the northern and north-western sector respect to the surface projection of the ruptured fault. These sectors correspond to azimuth between N320 and N40 roughly from the epicentre. Analogously, blue crosses correspond to stations in the western and southern sectors, at azimuth between N40 and N320 from the epicentre. Sites indicated through cross symbols correspond to "A" and "B" classes as defined by the Italian seismic code (NTC08). "A" sites correspond to Vs_{30}> 800 m/s, while "B" sites to 360 m/s < Vs_{30}< 800 m/s. We also add sites related to lower velocity values belonging to "C" (180 m/s < Vs_{30}< 360 m/s) and "D" sites (Vs_{30}< 180 m/s) that are depicted through crossed-dots. All GMPEs are plotted for "A/B" soil (Vs_{30} =760 m/s) and normal fault conditions.

Among the GMPEs used in this study, it is observed that the recorded ground motion parameters show better agreement with ITA10 and MAL11 model than the BA08 at almost all distances. However, the MAL11 matches better to trend of the observed ground accelerations at larger distances. In fact the recorded ground motions (PGAs, PGVs and SA) decay faster than the global empirical ground motion equations (BA08) as well as the ITA10 at larger distances. However, this feature is captured by the MAL11 model derived from the regional earthquake data in which the anelastic attenuation behavior is better determined. We found that there is a tendency for the three GMPEs to underestimate observed PGV and PGA levels at stations located in the northern and north-western sector and to overestimate observed values at sites in the eastern

and southern sectors. This feature suggests a role of directivity effects implying that stations in the north-western sector would correspond to the forward directivity area.

III. DIRECTIVITY EFFECT

For the purpose of investigating the role of directivity in the observed spatial distribution of maximum ground motion levels, and the differences of observed PGA and PGV values at comparable distances, we calculate the ratio between the observed PGA and PGV and the corresponding predicted values obtained from ITA10 GMPEs (PGA_{OBS}/PGA_{ITA10} and PGV_{OBS}/PGV_{ITA10}). These ratios for both PGA and PGV are plotted in **Figures 3a** and **4a**, respectively. Red symbols refer to ratios larger than 1 (i.e. empirical relations underestimate observations), while blue symbols are related to ratios lower than 1 (i.e. empirical relations overestimate observations). Both PGA and PGV spatial distribution show that in the north and north-western sector of the epicentre there is a predominance of ratio values higher than 1. These observations are in agreement with Cirella & Piatanesi (2016) kinematic rupture model confirming the rupture directivity towards north-west in the direction where the largest slip patch is associated with larger rupture velocity. In **Figures 3b** and **4b** PGA and PGV ratio values are plotted as a function of the azimuth in a modified geographic reference system. We rotated the geographic reference system by 32 degrees counter clockwise, in order to refer the azimuthal distance of stations to the fault strike direction, the new reference system origin corresponding to the epicentre of the main shock (we add white lines in **Figures 3a** and **4a** to visually show the reference system rotation). We use blue symbols for stations associated to "A" and "B" sites and red symbols for sites "C" and "D". PGA ratios systematically show larger in the north and north-western sectors of the epicentre, and lower values in the south-western sectors. The same behaviour characterizes the PGV ratios. These findings regarding directivity effects on the high frequency ground motion are in agreement

with many recent papers on recent Italian moderate-magnitude earthquakes occurred in 1997 in the Umbria-Marche region (Pino et al., 1999; Cultrera et al., 2008) in 2002 in Molise region (Gorini et al., 2004) and in 2009 L'Aquila earthquake (e.g. Malagnini et al., 2009, Akinci et al., 2010, Tinti et al., 2014, Calderoni et al., 2015). Interestingly in the south-south eastern area we observe an increase of PGA and PGV ratios, suggesting a bilateral rupture.

This inference is in agreement with Calderoni et al. (2016) recent findings that analysed the main shock records at 14 stations with different back-azimuth. They calculated the spectral ratios of the main shock and two smaller magnitude earthquakes localized in the same area providing a correction for the crustal attenuation variation. They inferred that the rupture mainly propagated towards NW with a lower slip release also towards SE.
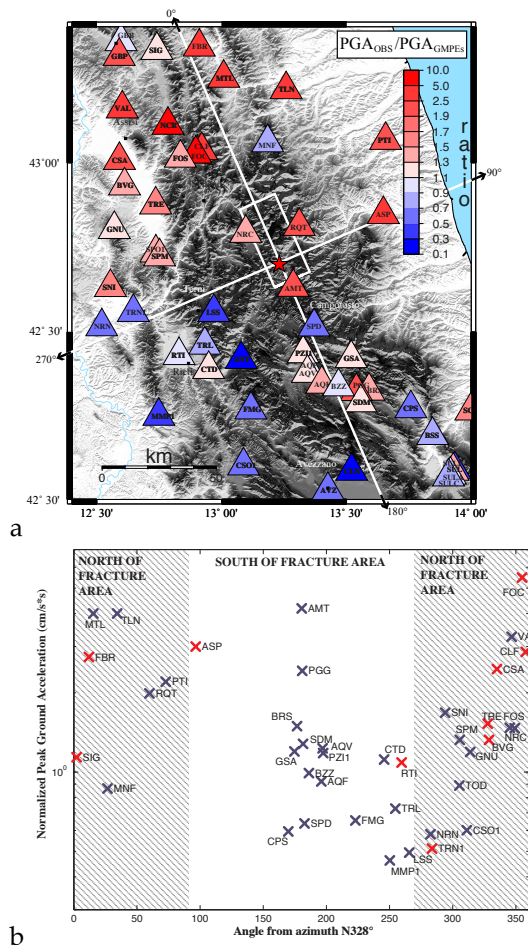
Figure 3. *(a) PGA ratio (PGAOBS/PGAITA10) areal distribution at the 98 considered stations of RAN. (b) PGA versus azimuth in a modified geographic reference system obtaining by rotating the geographic North of 32 degrees counter clockwise (white lines). Blue symbol indicates "A" and "B" site, red symbol refers to "C" and "D" sites.*
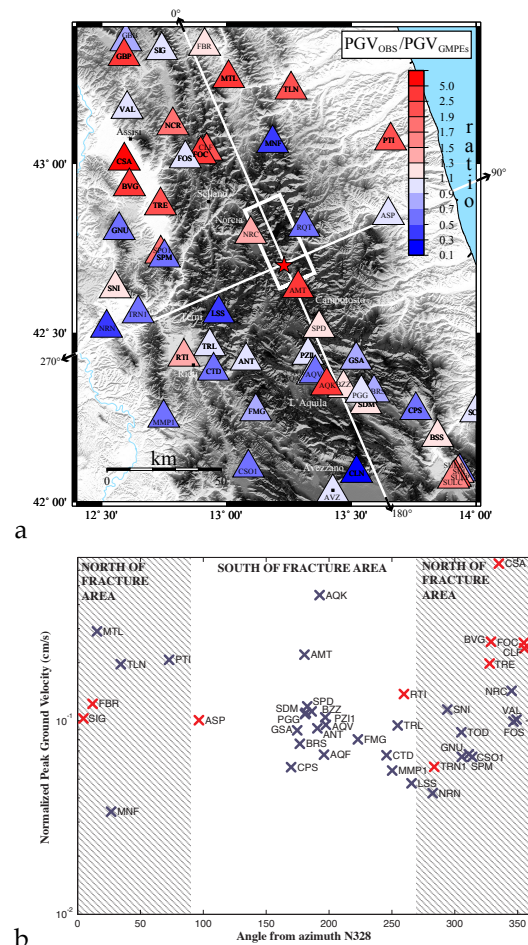
Figure 4. *(a) PGV ratio (PGV_{OBS}/PGV_{ITA10}) areal distribution at the 98 considered stations of RAN and (b) PGV versus azimuth in a modified geographic reference system, similarly to Figure 3.*

5
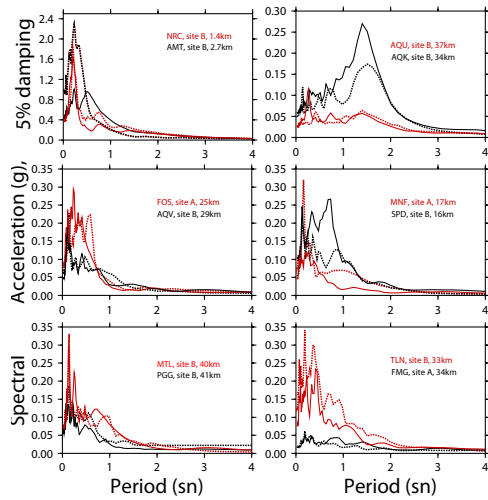
Figure 5. *Comparison of the acceleration response spectra at 5% damping ratio for two horizontal components (EW dashed line and NS solid line) registered at the stations that are located in forward (red lines) and backward (black lines) directivity sectors.*

In **Figure 5** we present the acceleration response spectra at 5% damping for the horizontal components (EW and NS) recorded at stations located both in the forward and backward directivity areas. At comparable R_{jb} distances, stations in the forward directivity sector show systematically higher spectral acceleration values. For example stations TLN, MTL, and FOS present larger ground accelerations than that of FMG, PGG and AQV, although showing similar distance and site condition. This discrepancy is attributed to rupture directivity, where the former stations are located in the forward directivity area, and the latter are in back forward directivity area. This effect is also pronounced in the higher periods (around 1 sec) presented at TLN and MTL acceleration spectra. For example, stations TLN and FMG are located at distances of R_{jb}=32 and 34 km, respectively. Station TLN shows peak ground acceleration (0.2 g) four times larger than station FMG (0.05 g) located in the backward directivity area.

Finally, we compare the spectral accelerations calculated at the near fault stations (e.g., AMT, NRC, MNF and SPD). The stations located at the southern area, AMT and SPD, have higher ground motions than that of northern stations (NRC, MNF) at periods, T > 0.5 sec. We interpret this feature as a small bilateral source rupture towards to south. Stations AMT and SPD are just located in the southern part of the nucleation point and the EW component of the station, parallel to the nodal plane, presents lower ground motions than the NS component. Stations AQU and AQK are both located in the backward directivity area at about the same distance and same site classification (Figure 5). Nevertheless, AQK station exhibits a larger level of ground acceleration around 0.25 g at 1.5 sec than AQU, ~0.1 g. Even though based on the Vs_{30} parameter the site conditions of station AQK indicate a class "B", this site demonstrates site amplification at about 0.6 Hz. This amplification is the effect of the impedance contrast occurring at depth larger than 30m in a sedimentary basin (e.g. De Luca et al, 1996; Akinci et al., 2010; Puglia et al., 2011).

IV. CONCLUSIONS

Comparison with empirical ground motion prediction illustrated that the observed ground motions seem coherent with ITA10 and region specific prediction equation MAL11 for short and medium periods. The observed ground motions are overestimated by the NGA, BA08 and ITA10 model at longer distances while it is better captured by the MAL11 model, derived from region specific database, which rigorously retains the anelastic attenuation parameter. This again emphasizes the importance of accessing specific regional seismic parameters for ground motion predictive equations (Akinci & Antonioli, 2013; Ugurhan et al. 2012).
The comparison between observed and predicted peak ground motions (PGA, PGV and SA) generally shows that the empirical predictions underestimate the observed values in the north-western sector and overestimate the observations in the SW area suggesting the source rupture related directivity effects.

PGA and PGV distributions were better investigated calculating the ratios with the corresponding predicted values obtained from ITA10 GMPEs (PGA_{OBS}/PGA_{ITA10} and PGV_{OBS}/PGV_{ITA10}) assuming invariant crustal attenuation properties in the study area. The trend of PGA and PGV ratios as a function of station azimuth confirmed the occurrence of a directivity effect towards NW direction and a systematic decrease of PGA and PGV at sites located in the SW sector. However, these findings are similar to those obtained by Lanzano et al., (2016) and Calderoni et al., (2016) in which the evident forward directivity effect has been recognized for the main shock through the analysis of the instrumental data caused by the fast rupture propagation towards NW direction along the seismogenic fault. In the SE sector we observe a slight increase of PGA and PGV ratios (e.g., AMT, SPD station) especially at the NS component that suggests a bilateral rupture, agreement with recent findings of Calderoni et al. (2016) and Spagnuolo et al. (2016).
We observed that station AQK does not present a regular behavior expected from a site classified with the "B" site category and presents large amplifications at larger periods at around 1.5 sec.

REFERENCES

[Akinci et al., 2010] Akinci, A., Malagnini, L., Sabetta, F. (2010). Characteristics of the strong ground motions from the 6 April 2009 L'Aquila earthquake, Italy. Soil Dyn. Earthq. Eng., 30: 320–335.

[Akinci & Antonioli, 2013] Akinci, A., Antonioli, A. (2013). Observations and stochastic modeling of 23 October 2011, M7.1 Van earthquake, Turkey, Geophys. J. Int. 192 (3), 1217–1239,
http://dx.doi.org/10.1093/gji/ggs075.

[Bindi et al., 2011] Bindi, D., Pacor, F., Luzi, L., Puglia, R., Massa, M., Ameri, G., Paolucci, R. (2011). Ground motion prediction equations derived from the Italian strong motion database. Bull Earthquake Eng (2011) 9:1899–1920 doi 10.1007/s10518-011-9313-z.

[Boore & Atkinson, 2008] Boore, D.M. and Atkinson, G.M., (2008). Ground-motion prediction equations for the average horizontal component of PGA, PGV, and 5 per cent-damped PSA at spectral periods between 0.01 s and 10.0 s. Earthq. Spectra, 24: 99–138.

[Calderoni et al., 2015] Calderoni, G., Rovelli, R., Ben-Zion, Y., Di Giovambattista, R. (2015). Along-strike rupture directivity of earthquakes of the 2009 L'Aquila, central Italy, seismic sequence. Geophys. J. Int., 203(1): 399–415.

[Calderoni et al., 2016] Calderoni, G., Rovelli, R., Di Giovambattista, R. (2016). Evidence of bilateral rupture in the Mw 6.0, Amatrice earthquake of 24 August 2016. DOI:10.5281/zenodo.61713

[Castelli et al., 2016] Castelli V., Camassi R., Caracciolo C., Locati M., Meletti C., Rovida A. (2016). New insights in the seismic history of Monti della Laga area. Annals of Geophysics, 59, Fast Track 5, 2016; DOI: 10.4401/ag-7243

[Cirella et al., 2016] Cirella A., and A. Piatanesi (2016). Source Complexity of the 2016 Amatrice Earthquake from Non Linear Inversion of Strong Motion Data: Preliminary Results; DOI:10.5281/zenodo.153821

[Cultrera et al., 2008] Cultrera C, Pacor F, Franceschina G, Emolo A, Cocco M. (2008). Directivity effect for moderate-magnitude earthquakes (Mw 5.6–6.0) during the 1997 Umbria–Marche sequence, central Italy. Tectonophysics, Tectonophysics, doi: 10.1016/j.tecto.2008.09.022

[De Luca et al., 2005] De Luca S, Marcucci G, Milana T, Sano' (2005). Evidence of low-frequency amplification in the City of L'Aquila, Central Italy, through a multidisciplinary approach including strong- and weak-motion data, ambient noise, and nu-

merical modeling. Bull. Seismol. Soc. Am., 95:1469–81.

[Gorini et al., 2004] Gorini A, Marcucci S, Marsan P, Milana G. (2004). Strong motion records of the 2002. Molise, Italy, earthquake sequence and stochastic simulation of the main shock. Earthquake Spectra 20(S1):S65–79.

[Gruppo di Lavoro INGV, 2016] Gruppo di Lavoro INGV sul terremoto di Amatrice (2016). Secondo rapporto di sintesi sul Terremoto di Amatrice Ml 6.0 del 24 Agosto 2016 (Italia Centrale), doi: 10.5281/zenodo.154400

[Lanzano et al., 2016] Lanzano G., Luzi L., Pacor F., Puglia R., D'Amico M., Felicetta C., Russo E. (2016). Preliminary analysis of the accelerometric recordings of the August 24th, 2016 MW 6.0 Amatrice earthquake Annals of Geophysics, 59, Fast Track 5, 2016 DOI: 10.4401/ag-7201

[Luzi et al., 2016] Luzi, L., Puglia, R., Russo, E., D'Amico, M., Felicetta, C., Pacor, F., Lanzano, G., Ceken, U., Clinton, J., Costa, G., Duni, L., Farzanegan, E., Gueguen, P., Ionescu, C., Kalogeras, I., Ozener, H., Pesaresi, D., Sleeman, R., Strollo, A. and Zare, M. (2016). The engineering strong-motion database: a platform to access Pan-European accelerometric data. Seismological Research Letters, 87(4):987- 997.

[Malagnini et al., 2011] Malagnini, L., Akinci, A., Mayeda, K., Munafo, I., Herrmann, R.B.,` Mercuri, A. (2011). Characterization of earthquake-induced ground motion from the L'Aquila seismic sequence of 2009, Italy. Geophys. J. Int., 184: 325–337.

[NTC, 2008] Italian building code 'Norme Tecniche per le Costruzioni – NTC08' Ministero delle Instrutture e dei Trasporti 2008

[Pino et al., 1999] Pino NA, Mazza S, Boschi E. (1999). Rupture directivity of the major shocks in the 1997 Umbria–Marche (central Italy) sequence from regional broad-

band waveforms. Geophys. Res. Lett., 26(14):2101–4.

[Puglia et al., 2011] Puglia R., Ditommaso R., Pacor F., Mucciarelli M., Luzi L., Bianca M. (2011). Frequency variation in site response as observed from strong motion data of the L'Aquila (2009) seismic sequence. Bull Earthquake Eng (2011) 9:869–892 DOI 10.1007/s10518-011-9266-2

[Scognamiglio et al., 2016] Scognamiglio L., E. Tinti, and M. Quintiliani, The 2016 Amatrice (Central Italy) seismic sequence: fast determination of time domain moment tensors and finite fault model analysis of the 02:33:29 UTC 24 August 2016 ML 5.4 aftershock (Submitted to Annals of Geophysics, this issue).

[Spaguolo et al., 2016] Spagnuolo. E., Cirella, A., Akinci, A. (2016). Investigating the effectiveness of rupture directivity during the Mw 6.0 Amatrice earthquake, central Italy (Submitted to Annals of Geophysics, this issue).

[Tinti et al., 2016] Tinti E., Scognamiglio L., Michelini A. and Cocco M. (2016). Slip heterogeneity and directivity of the ML 6.0, 2016, Amatrice earthquake estimated with rapid finite-fault inversion. Geophys. Res. Lett., 43, 10,745–10,752, doi:10.1002/2016GL071263.

[Ugurhan et al. 2012] Ugurhan, B., Aysegul, A., Akinci, A., Malagnini, L. (2012). Strong-Ground Motion Simulation of the 6 April 2009 L'Aquila, Italy, Earthquake. Bull. Seism. Soc. Am., 102(4): 1429-1445.